Biology Division, Indian Institute of Science Education and Research (IISER), Pune
Central Tower, Sai Trinity Building, Sutarwadi, Pashan, Pune-21, India

INVESTIGATING DYNAMICS OF CHECKPOINT ACTIVATION IN RESPONSE TO DNA ALKYLATION DAMAGE IN BREAST EPITHELIAL CELLS

Surojit Sural

Reg. No. 20071006, IISER Pune

A thesis submitted in partial fulfillment of the requirements

for the BS-MS dual degree programme in IISER Pune

Research Advisor:

Dr. Mayurika Lahiri, Assistant Professor

Biology Division, IISER Pune

Certificate

This is to certify that this dissertation entitled 'Investigating dynamics of checkpoint activation in response to DNA alkylation damage in breast epithelial cells' towards the partial fulfillment of the BS-MS dual degree programme at the Indian Institute of Science Education and Research (IISER), Pune represents original research carried out by Surojit Sural at IISER Pune under the supervision of Dr. Mayurika Lahiri, Assistant Professor, Biology Division, IISER Pune during the academic year 2011-2012.

Dr. Mayurika Lahiri

Assistant Professor

Biology Division, IISER Pune

Declaration

I hereby declare that the matter embodied in the thesis entitled 'Investigating dynamics of checkpoint activation in response to DNA alkylation damage in breast epithelial cells' are the results of the investigations carried out by me at the Biology Division, IISER Pune under the supervision of Dr. Mayurika Lahiri, Assistant Professor, Biology Division, IISER Pune and the same has not been submitted elsewhere for any other degree.

Surojit Sural

BS-MS Dual Degree Student

IISER Pune

Abstract

N-nitroso-N-methylurea (MNU) is an S_N1 type DNA methylating agent which forms the modified base O^6-methylguanine. Two major pathways involved in mediating DNA damage response in mammalian cells are ATM through Chk2 for double-strand breaks and ATR through Chk1 for single-strand breaks or stalled replication forks. We investigated the dynamics of checkpoint activation in breast adenocarcinoma-derived MCF7 cells at different concentrations of MNU and found a correlation between degradation of the suicidal repair enzyme O^6-methylguanine DNA methyltransferase (MGMT) and activation of the DNA damage signaling pathways. ATM phosphorylation was detected at all MNU doses; however phosphorylation of effector kinases, Chk1 and Chk2, was observed only at lower MNU concentrations. Interestingly, at higher doses of MNU, activation of caspase 9 occurred in absence of Chk1 and Chk2 phosphorylation. MCF10A cells of normal breast epithelial origin and MGMT-depleted MCF7 cells showed activation of DNA damage checkpoint kinases at a much lower MNU concentration in comparison with MCF7 cells. ATM, Chk2 and Chk1 were phosphorylated at the same time point after induction of MNU damage; however for damage induced by the DNA ethylating agent N-nitroso-N-ethylurea (NEU), ATM and Chk2 phosphorylation preceded Chk1 phosphorylation. Interestingly, Chk1 phosphorylation induced after NEU damage was independent of ATM and DNA-PK activation. We have also established a 3-dimensional basement membrane culture of MCF10A cells to investigate early tumorigenic effects of MNU-induced damage during different stages of development of human mammary acini.

Table of Contents

List of Figures

Acknowledgements

Since I worked in a common lab for my BS-MS thesis project, the acknowledgement section has to be the most elaborate one. I thank my thesis advisor, Dr. Mayurika Lahiri, for her support and supervision during my three years in her research group. I sincerely acknowledge her for encouraging me to independently design primary aspects of this project. I thank my thesis advisory committee members, Dr. Aurnab Ghose and Dr. Nagaraj Balasubramanian, for discussions which were very helpful in expanding my forte of experimental techniques, especially 3D culture and microscopy. I would also like to thank Dr. Richa Rikhy, Dr. Thomas Pucadyil and Dr. N. K. Subhedar for providing necessary reagents for my experiments from their respective labs.

I thank Prasad for standardizing protocols of the nitroso compound project which made life much easier for me. Special thanks to Satish for repeating quite a lot of my experiments which further strengthened the credibility of my 'interesting' results. I would like to thank Mitali, Payal, Abhinav and other Lahiri lab members for their valuable inputs during weekly lab meetings. Thanks to Vijay, Varsha and Abhishek for their help in acquisition and analysis of confocal microscopy images. I still remember my excitement when I first observed a hollow multicellular structure under the microscope.

Special thanks to my parents and sister for their eternal support and for never letting me be affected by the hardships they had to endure during my academic journey. I would also thank some special persons in my life for making me feel strong and important in the last one year. Thanks to my three batchmates, Manoj, Sarthak and Guhan, for the refreshing conversations we had at the end of tiring days at work. I thank the IISER authorities for segregating the 2007 batch from the rest of IISER in the final year of our course; this endowed us with the liberty we needed to discover our interests in life.

I would like to thank Kishore Vaigyanik Protsahan Yojana (KVPY), Bangalore for providing financial support throughout my academic endeavor. I also thank Christian Medical College (CMC), Vellore for granting a travel award to attend the Tenth CMC Winter Symposium on Cellular and Molecular Medicine.

Finally, I thank the Biology Division at IISER Pune for funding the experiments of my thesis project and for providing the most wonderful environment for undergraduate research in the country.

Introduction

DNA damage checkpoint signaling in mammalian cells

Eukaryotic genomes are under continuous assault by exogenous agents and byproducts of intracellular metabolism. To preserve the genomic integrity, cells employ complex surveillance mechanisms, called checkpoints, which counteract these omnipresent DNA-damaging effects. The overall function of these checkpoints is to detect damaged DNA, and to coordinate DNA repair, cell cycle arrest and/or apoptosis. This phenomenon comprises a multistep cascade which involves sensing the DNA damage, activation of apical protein kinase(s), signal amplification through downstream kinase(s), and activation of effector proteins which eventually regulate several cellular-level responses (Figure **1**). The sensor or apical kinases which detect the damaged DNA belong to the phosphoinositide 3-kinase related kinase (PIKK) family. These kinases, namely ATM (ataxia-telangiectasia mutated) and ATR (ATM and Rad 3-related), initiate a cascade of phosphorylation events which mediate cell cycle arrest, DNA repair and apoptosis (Ciccia and Elledge, 2010). The increased local concentration of ATM at the double strand break (DSB) site is important to boost phosphorylation of ATM targets, including signal mediators such as the Chk2 kinase (Shiloh, 2006). ATR responds primarily to stalled replication forks, base adducts and DNA cross-links, and relays the signal by phosphorylating Chk1 kinase and a large subset of ATM substrates (Cimprich and Cortez, 2008). However this paradigm of ATM and ATR signalling through two independent and alternate pathways was recently challenged and redefined by several reports showing that ATR can be activated directly in response to DSBs specifically in S and G_2 phases of the cell cycle (Jazayeri et al., 2006; Helt et al., 2005). Recruitment of ATR to ionising radiation (IR)-induced DSBs occurs in an ATM and Mre11-Rad50-Nbs1 (MRN) complex-dependent manner at time points following ATM activation (Adams et al., 2006). The ATM–to–ATR switch is driven by DSB resection mediated by MRN-CtIP and Exo1 exonucleases which leads to homologous recombination (HR)-mediated DSB repair (Shiotani and Zou, 2009).

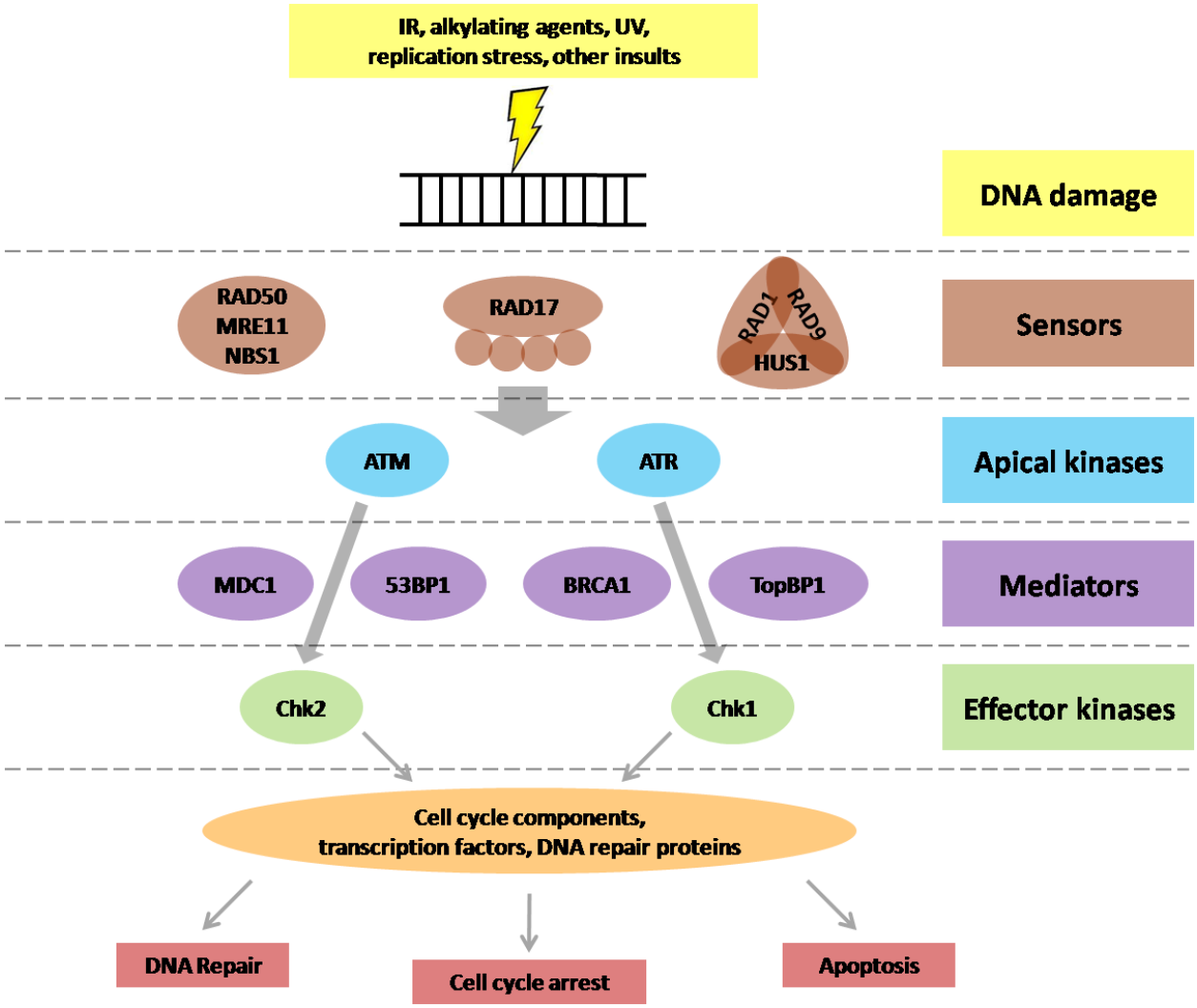

Figure 1. Schematic representation of mammalian DNA damage checkpoint signaling cascade. DNA damage is sensed by sensor protein complexes which results in activation of apical kinases, ATM and ATR. The signal is transduced to effector kinases, Chk2 and Chk1 respectively, which in turn phosphorylate downstream substrates and regulate the cellular response to DNA damage. Mediator proteins interact with damage sensors, signal transducers and effector proteins in a cell cycle dependent manner and thus maintain the specificity of this signal transduction cascade.

DNA damage induced by monofunctional alkylating agents

Alkylating agents are a structurally diverse group of DNA damaging agents which form adducts at ring nitrogen (N) and extracyclic oxygen (O) atoms of DNA bases (Shrivastav et al., 2010). N-nitroso-N-methylurea (MNU), a simple monofunctional S_N1 type DNA methylating agent, forms the modified base O^6-methylguanine (O^6meG) which mispairs with thymine during DNA replication (Kondo et al., 2010). This lesion can potentially result in a G:C→A:T transition mutation after two cycles of DNA replication (**Figure 2**). Similarly, N-nitroso-N-ethylurea (NEU), a monofunctional S_N1 type DNA ethylating agent, forms the modified base O^6-ethylguanine (O^6EtG) which also primarily induces G:C→A:T transitions (Engelbergs et al., 2000). These compounds are prototypical of a family of O^6-alkylating agents used in cancer chemotherapy for almost 30 years (Kaina et al., 2010). Cells possess a suicidal repair enzyme, O^6-methylguanine DNA methyltransferase (MGMT), which repairs O^6-meG lesions by transferring the methyl moiety to an internal cystiene-145 residue and targets itself to proteosomal degradation (Xu-Welliver and Pegg, 2002). MGMT overexpression in certain cancers, such as gliomas, renders resistance to O^6-alkylating drugs and hence several inhibitors of MGMT are used in clinical trials to improve the therapeutic efficacy of these anticancer agents (Kaina et al., 2010). At higher doses of DNA alkylating agents, the mismatch repair (MMR) proteins, namely Msh2–Msh6 and Mlh1–Pms2 heterodimers, play a pivotal role in mediating the cytotoxic effects of O^6-meG lesions (Christmann and Kaina, 2000). *Mgmt*$^{-/-}$ *Msh6*$^{-/-}$ and *Mgmt*$^{-/-}$ *Mlh1*$^{-/-}$ mice are much more alkylation-resistant than *Mgmt*-null mice (Klapacz et al., 2009), however the mechanisms leading to MMR-induced apoptosis after treatment with O^6-alkylating agents are still controversial. According to one model, O^6-meG:T mismatches formed after DNA replication are recognized by the MMR system which invokes excision of the nucleotide opposite to the O^6-meG lesion. Due to erroneous base pairing properties of O^6-meG, a thymine is reinserted at the site thus leading to a futile cycle of MMR-induced excision and repair (Fu et al., 2012). A combination of these recurring single-stranded DNA gaps and DSBs that may possibly form during the next replication cycle might cause activation of the DNA damage checkpoint (**Figure 2**). However according to an alternate model, the recognition of O^6-meG:T mispairs by the MMR proteins have been shown to directly

recruit ATR kinase to the site of DNA damage which elicits cell cycle checkpoint activation and apoptosis (Liu et al., 2010).

MNU-induced rat mammary tumor model

In addition to its use as a chemotherapeutic agent, MNU can be used to experimentally induce mammary gland tumors in female rats (Takahashi et al., 1995). The rat mammary tumor model has been traditionally used to study different stages of mammary carcinogenesis due to its morphological and gene expression profile similarities with low-to-intermediate grade breast cancer in humans (Chan et al., 2005; Russo and Russo, 2000). However there are numerous limitations to this animal model since it is not amenable for investigating cellular signaling pathways responsible for progression of early stages of oncogenesis.

Specific aims of this study

To understand the overall response of human mammary epithelial cells to S_N1 type DNA alkylating agents, we investigated the activation of DNA damage checkpoint pathways after brief exposure to different doses of these compounds. We also focused on two established responses to O^6meG lesions, MGMT-mediated repair and activation of apoptotic caspases, and how they are correlated with phosphorylation of different upstream kinases in the checkpoint signaling cascade. Since it is still controversial whether ATM or ATR kinases are directly recruited to the damaged sites induced by monofunctional alkylating agents, we investigated the temporal dynamics of activation of the canonical DNA damage response pathways and their interdependence for signal transduction to downstream cellular targets. Finally, we developed a three-dimensional (3D) culture model of human glandular epithelial cells (MCF10A) which can be used as a powerful tool to investigate early molecular events in MNU-induced mammary carcinogenesis.

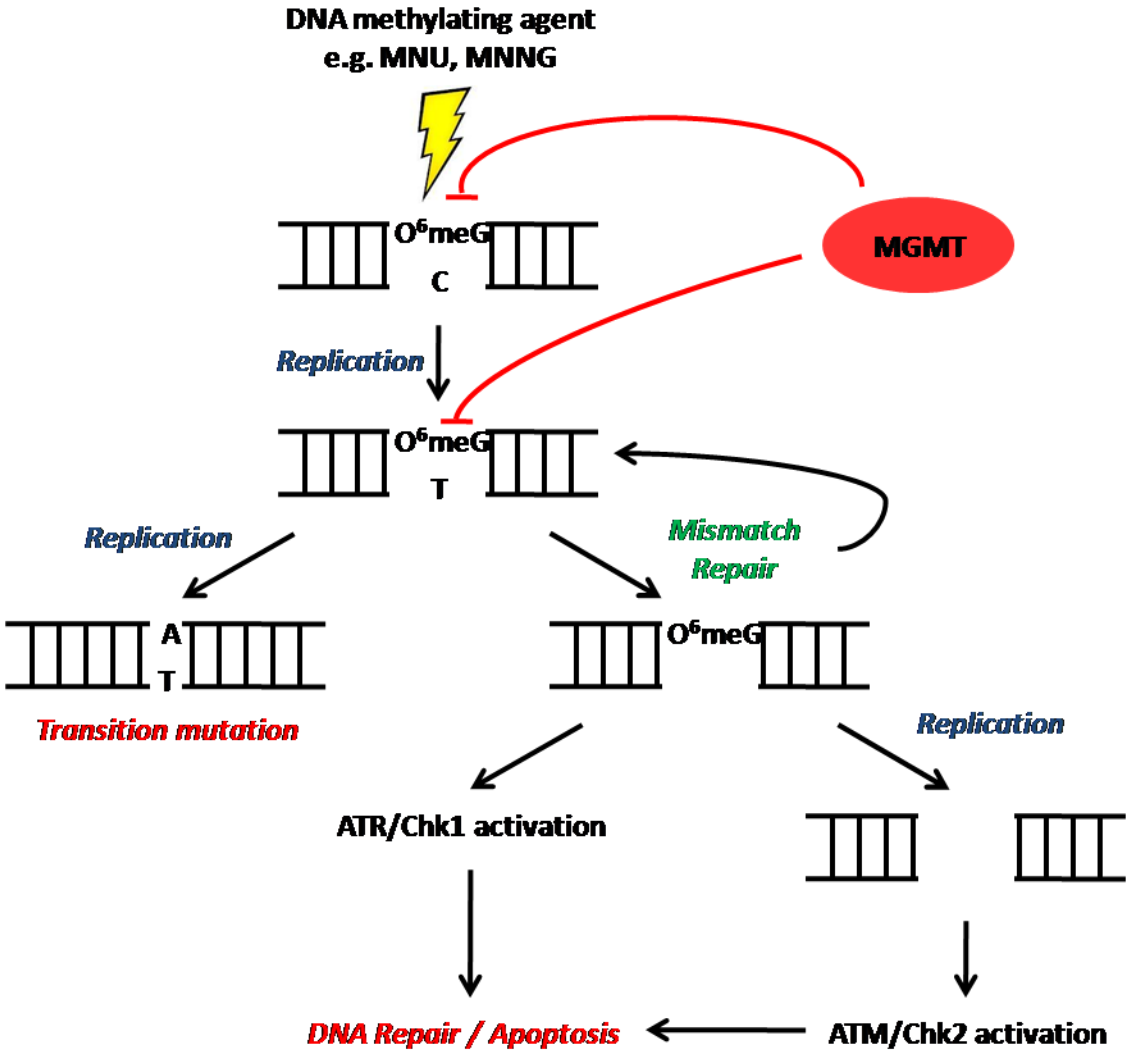

Figure 2. Biological effects of DNA methylating agents. Monofunctional DNA methylating agents lead to the formation of *O*^{6}meG adducts which are repaired by the DNA repair enzyme, MGMT. If left unrepaired, *O*^{6}meG mispairs with T during DNA replication which results in a G:C→A:T transition mutation in the subsequent round of replication. MMR system recognizes *O*^{6}meG:T and *O*^{6}meG:C mismatches and leads to a futile repair cycle thus generating an active SSB lesion at the damage site. If MMR single strand intermediates bypass the cell cycle arrest, this results in formation of a DSB lesion in the next replication phase which activates the cell cycle checkpoint signaling cascade.

Materials and Methods

Chemicals and antibodies

Dimethyl sulfoxide (DMSO), N-nitroso-N-methylurea (MNU), N-nitroso-N-ethylurea (NEU), O6-benzylguanine (O6-BG), epidermal growth factor (EGF), hydrocortisone, cholera toxin from *Vibrio cholera*, insulin from bovine pancreas, thiazolyl blue tetrazolium bromide (MTT), thymidine, 2-Amino-2-(hydroxymethyl)-1,3-propanediol (Tris), glycerol, bromophenol blue, 1,4-Dithioerythritol (DTE), acrylamide, N,N'-methylenebisacrylamide, sodium dodecyl sulfate (SDS), ammonium persulfate (APS), N,N,N′,N′-tetramethylethylenediamine (TEMED), sodium chloride, ethylenediaminetetraacetic acid (EDTA), sodium orthovanadate, sodium fluoride, sodium azide, protease inhibitor cocktail for mammalian cell and tissue extracts, Triton-X-100, Tween 20 and N-propyl gallate were all purchased from Sigma-Aldrich. Glycine, sodium hydroxide, potassium chloride, hydrochloric acid and methanol were obtained from Fisher Scientific. Paraformaldehyde (PFA) was bought from J.T.Baker. Bovine serum albumin (BSA) was purchased from Himedia. Selective ATM inhibitor KU 55933, DNA-PK inhibitor DMNB and Mre11 inhibitor Mirin were obtained from Tocris Bioscience. Precision Plus Protein Dual Color Standards were purchased from Bio-Rad. Monoclonal Chk1 antibody and polyclonal Exo1 antibody were bought from Santa Cruz Biotechnology. Polyclonal antibodies for phospho-Chk1 (Ser345), phospho-Chk2 (Thr68) and monoclonal Chk2 antibody were purchased from Cell Signaling Technology. Polyclonal active caspase 9 antibody and monoclonal antibodies for phospho ATM (Ser1981) and ATM were obtained from Abcam. Monoclonal antibodies for MGMT and α-tubulin were bought from Sigma. Monoclonal antibodies for α6-integrin and β-catenin were purchased from Millipore and BD Biosciences, respectively. AffiniPure F(ab')$_2$ fragment goat anti-mouse IgG and peroxidase-conjugated AffiniPure goat anti-mouse and anti-rabbit IgG (H+L) were obtained from Jackson Immuno Research. 4′,6-Diamidino-2-phenylindole dihydrochloride (DAPI), Alexa Fluor 488 and 594 donkey anti-rat and 488 and 568 goat anti-mouse IgG (H+L) were bought from Invitrogen.

Cell lines and culture conditions

MCF7 cell line was purchased from European Collection of Cell Cultures (ECACC). HeLa and MCF10A cell lines were generous gifts from Dr. Sorab Dalal (ACTREC, Mumbai) and Prof. Raymond C. Stevens (The Scripps Research Institute, California), respectively. MCF7 and HeLa cells were grown in High Glucose Dulbecco's Modified Eagle Medium (DMEM; Invitrogen or Lonza) containing 10% fetal bovine serum (FBS; Invitrogen), 2 mM L-glutamine (Invitrogen) and 1X Antibiotic-Antimycotic (Invitrogen). MCF10A cells were grown in High Glucose DMEM without sodium pyruvate (Invitrogen) containing 5% horse serum (Invitrogen), 20 ng/mL EGF, 0.5 µg/mL hydrocortisone, 100 ng/mL cholera toxin, 10 µg/mL insulin and 100 units/mL penicillin-streptomycin (Invitrogen) and were resuspended during sub-culturing in High Glucose DMEM without sodium pyruvate containing 20% horse serum and 100 units/mL penicillin-streptomycin (Invitrogen). All cell lines were maintained in 100 mm tissue-culture treated dishes (Corning) at 37°C in humidified 5% CO_2 incubator (Thermo Scientific). For long term storage in liquid nitrogen, MCF7 and HeLa cells were stored in DMEM containing 10% DMSO and 20% FBS and MCF10A cells were stored in DMEM containing 5% DMSO and 10% FBS.

MTT-based cytotoxicity assay

MCF7 cells were seeded at a density of 10^4 cells per well in 96-well flat bottom tissue-culture treated plates (Corning) and maintained at 37°C for 16 hours. Cells were then treated with different concentrations of MNU (ranging from 0.2 to 20 mM) for 2 hours. Medium containing drug was aspirated and cells were fed with fresh growth medium containing 0.5 mg/mL MTT. Plates were wrapped in aluminium foil and maintained at 37°C for 4 hours. Medium-MTT mixture was aspirated from wells and MTT-formazan crystals were dissolved in 100 µL DMSO. Plates were kept on a nutating shaker at room temperature (RT) for 5 minutes and absorbance was recorded at 570 nm using a Varioskan Flash Multimode Plate Reader (Thermo Scientific).

Drug treatment and time course assays

Cells were seeded at a density of 10^6 cells per well in 6-well tissue-culture treated plates (Corning) and maintained at 37°C for 16 hours. Cells were then treated with different concentrations of MNU or NEU for 2 hours (unless otherwise indicated). Control cells were treated with equivalent volume of DMSO (drug solvent). For time course studies, cells were treated with drug for different time periods ranging from 0 to 120 minutes. For MGMT and Mre11 inhibition studies, cells were treated with 20 µM O6-BG and 25 or 100 µM Mirin, respectively, one hour prior to drug treatment. For ATM and DNA-PK inhibition, cells were treated with 10 µM KU 55933 and 25 µM DMNB, respectively, immediately prior to addition of drug. After drug treatment, medium containing drug was aspirated and cells were washed once with 1X phosphate buffered saline (PBS; PAN-Biotech GmbH). Cells were lysed in 1X sample buffer containing 0.06 mM Tris (pH 6.8), 6% glycerol, 2% SDS, 0.1 M DTE and 0.006% bromophenol blue and lysates were stored at -40°C.

Immunoblot analysis

Cell lysates in 1X sample buffer were heated at 95°C and spun at 12,100 X g for 1 minute at RT. Sodium dodecyl sulphate polyacrylamide gel electrophoresis (SDS-PAGE) apparatus was set up using a SE 260 mini-vertical gel electrophoresis unit (GE Healthcare) using the manufacturer's protocol. SDS-PAGE gels were prepared using 6-15% resolving gel (5.8-14.5% acrylamide, 0.2-0.5% bisacrylamide, 475 mM Tris, pH 8.8, 0.1% SDS, 0.1% APS and 0.04-0.08% (v/v) TEMED) and 5% stacking gel (4.93% acrylamide, 0.07% bisacrylamide, 125 mM Tris, pH 6.8, 0.1% SDS, 0.1% APS and 0.1% [v/v] TEMED). Samples were loaded onto gels and resolved at 100 V for 3 hours. Blot transfer was set up using Immobilon-P polyvinyldifluoride (PVDF) membranes (Millipore) in TE22 mighty small transphor unit (GE Healthcare) at 115 mA for 16 hours. Blocking was performed by incubating the blots in 5% (w/v) skimmed milk (SACO Foods, US) for non-phospho antibodies or 4% (w/v) Block Ace (AbD Serotec) for phospho-specific antibodies prepared in 1X tris buffered saline (TBS; 25 mM Tris (pH 7.6), 150 mM NaCl and 2 mM KCl) containing 0.1% Tween 20 (1X TBS-T) for 1 hour at RT with gentle rocking. Blots were incubated for 3 hours at RT (or for 16 hours at 4°C)

with gentle rocking in primary antibody solution, phospho Chk1 Ser345 (1:5000), Chk1 (1:2500), phospho Chk2 Thr68 (1:2500), Chk2 (1:2500), phospho ATM Ser1981 (1:2000), ATM (1:1000), active Caspase 9 (1:500), MGMT (1:1000), Exo1 (1:1000), α6-integrin (1:1000), β-catenin (1:2500) and α-tubulin (1:20000); prepared in blocking solution. Blots were washed four times with 1X TBS-T and incubated with peroxidase-conjugated secondary antibody solution (1:10000) prepared in 5% (w/v) skimmed milk in 1X TBS-T for 1 hour at RT with gentle rocking. Blots were washed four times with 1X TBS-T, developed using Immobilon Western Detection Reagent kit (Millipore) and visualized using Fuji LAS 4000 (GE Healthcare).

3D on-top culture

Wells in 24-well tissue-culture treated plates were coated with 120 µL growth factor reduced basement membrane matrix (or Matrigel; BD Biosciences) and allowed to gel at 37°C for 15 minutes. MCF7 cells suspended in DMEM were seeded at a density of 0.4 X 10^5 cells per well on top of Matrigel coat and after 30 minutes an equal volume of DMEM containing 10% (v/v) Matrigel was added to the wells. Cultures were maintained for 8 days at 37°C and DMEM containing 5% Matrigel was supplemented every 2 days (Lee et al., 2007). For drug treatments, MNU or NEU was directly added to the culture medium. For MCF10A cells, cell suspension was prepared in assay medium (DMEM containing 2% horse serum, 0.5 µg/mL hydrocortisone, 100 ng/mL cholera toxin, 10 µg/mL insulin and 100 units/mL penicillin-streptomycin) supplemented with 2% Matrigel and 5 ng/mL EGF. This suspension was added on top of 120 µL Matrigel coat to attain a cell density of 0.4 X 10^5 cells per well in 24-well tissue-culture treated plates. Cultures were maintained for 10 days at 37°C and assay medium containing 2% Matrigel and 5 ng/mL EGF was supplemented every 4 days (Debnath et al., 2003). For drug treatments, MNU or NEU was directly added to the culture medium.

In-well 3D culture extraction and immunofluorescence

Medium was aspirated from 3D on-top cultures and wells were rinsed twice with ice-cold PBS. 2-3 times the medium volume of ice-cold PBS-EDTA (PBS containing 5 mM EDTA, 1 mM sodium orthovanadate, 1.5 mM sodium fluoride and 1X protease inhibitor

cocktail) was added to the wells and Matrigel was detached from the bottom of culture surface. Plates were incubated at 4°C for 30 minutes with gentle rocking and majority of supernatant was aspirated. 3D structures were placed on glass slides (Thermo Scientific) and allowed to adhere for 15 minutes at RT. Slides were fixed using 4% PFA (freshly prepared in PBS, pH 7.4) for 10 minutes at RT and washed four times with 1X PBS-Glycine (PBS containing 100 mM glycine) for 10 minutes at RT. Cultures were permeabilized using PBS containing 0.5% Triton-X-100 for 5 minutes and were washed three times with immunofluorescence (IF) buffer (PBS containing 0.05% [w/v] sodium azide, 0.1% [w/v] BSA, 0.2% [v/v] Triton-X-100 and 0.05% Tween 20) for 10 minutes at RT. Slides were first blocked with primary blocking solution (10% [v/v] goat serum [Abcam] in IF buffer) for 90 minutes at RT and then with secondary blocking solution (IF buffer containing 10% goat serum and 1% $F(ab')_2$ fragment goat anti-mouse IgG) for 45 minutes at RT in a humid chamber. Cultures were stained with primary antibody prepared in secondary blocking solution, α6-integrin (1:100) or β-catenin (1:100); for 16 hours at 4°C in a humid chamber. Slides were washed three times with IF buffer for 20 minutes at RT. Cultures were incubated with secondary antibody prepared in secondary blocking solution, Alexa 488 and 594 conjugated donkey anti-rat (1:200) and Alexa 488 and 568 conjugated goat anti-mouse IgG (1:200); for 60 minutes at RT in a humid chamber. Slides were washed three times with IF buffer for 20 minutes and once with PBS for 10 minutes at RT. Cultures were counterstained with PBS containing 0.5 µg/ml DAPI for 10 minutes and slides were washed with PBS for 10 minutes at RT. Slides were mounted with mounting medium (20 mM Tris [pH 8.0], 0.5% [w/v] N-propyl gallate and 90% [v/v] glycerol) using 22 X 30 mm cover glass (Micro Aid) and were allowed to set overnight at 4°C. 3D structures were visualized under a Zeiss LSM 710 laser scanning confocal microscope. All immunofluorescence images, unless otherwise specified, were captured using 63X oil-immersion objective.

Results

MNU causes dose-dependent checkpoint activation in MCF7 cells

MTT-based cytotoxicity assay was performed to investigate cell viability after 2 hours of MNU damage to MCF7 cells (a cell line derived from mammary adenocarcinoma). Cell viability decreased exponentially after MNU treatment and LD_{50} value was obtained to be 6 mM (Figure **3**). Cells were treated with different MNU doses (3 mM to 15 mM) to encompass a cytotoxicity range from 100% cell viability to 75% cell death. Phosphorylation of sensor kinase ATM at serine-1981 residue was detected at all MNU doses from 3 mM to 15 mM (Figure **4**). Interestingly, phosphorylation of effector kinases, Chk2 and Chk1, were detected only at intermediate MNU doses (3 mM to 9 mM; Figure **4**) and in this range, the degree of phosphorylation decreased with increase in MNU concentration. Activation of caspase 9 was observed for MNU concentrations higher than 9 mM and interestingly, in the absence of the activation of effector kinases, Chk2 and Chk1 (Figure **4**). MGMT levels declined drastically in MCF7 cells treated with MNU (Figure **4**).

To further elucidate the MNU dose-dependent activation of checkpoint proteins, MCF7 cells were treated with MNU doses ranging between 0.5 mM and 5 mM. Chk1 phosphorylation was detected at a lower MNU concentration (2 mM) in comparison to the dose at which ATM or Chk2 phosphorylation were detected (3 mM; Figure **5**). MGMT levels declined rapidly with increase in MNU concentration and interestingly, decline in MGMT levels correlated with increase in phosphorylation of effector kinases, Chk2 and Chk1 (Figure **5**). Activation of caspase 9 was not detected in this range of MNU doses (Figure **5**).

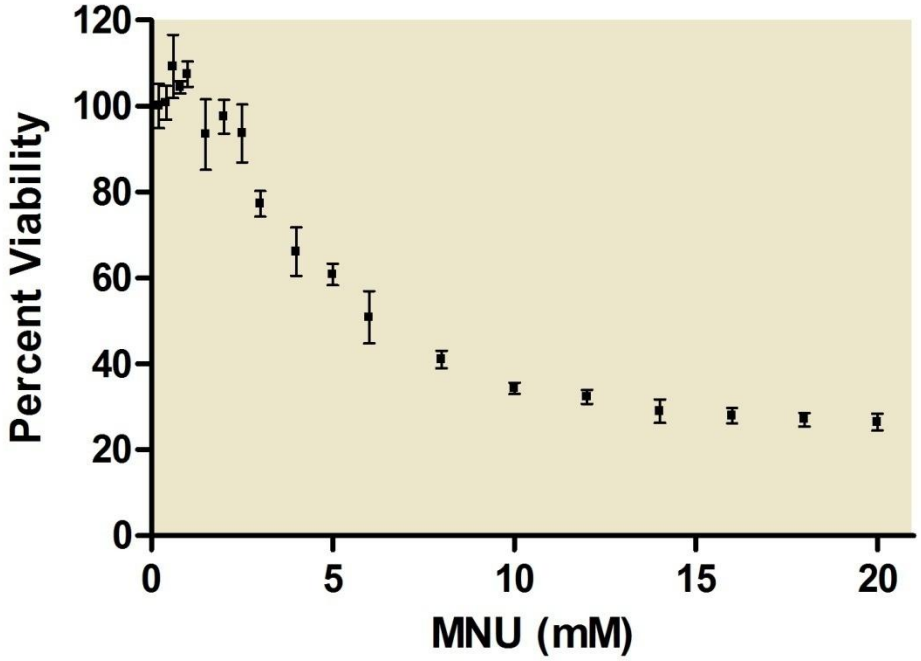

Figure 3. MTT-based cytotoxicity assay in MCF7 for different MNU doses. Cells were treated with MNU concentrations ranging between 0.2 mM and 20 mM for 2 hours. Percent viability was determined for each MNU dose by normalizing corresponding absorbance at 570 nm with respect to that for untreated cells.

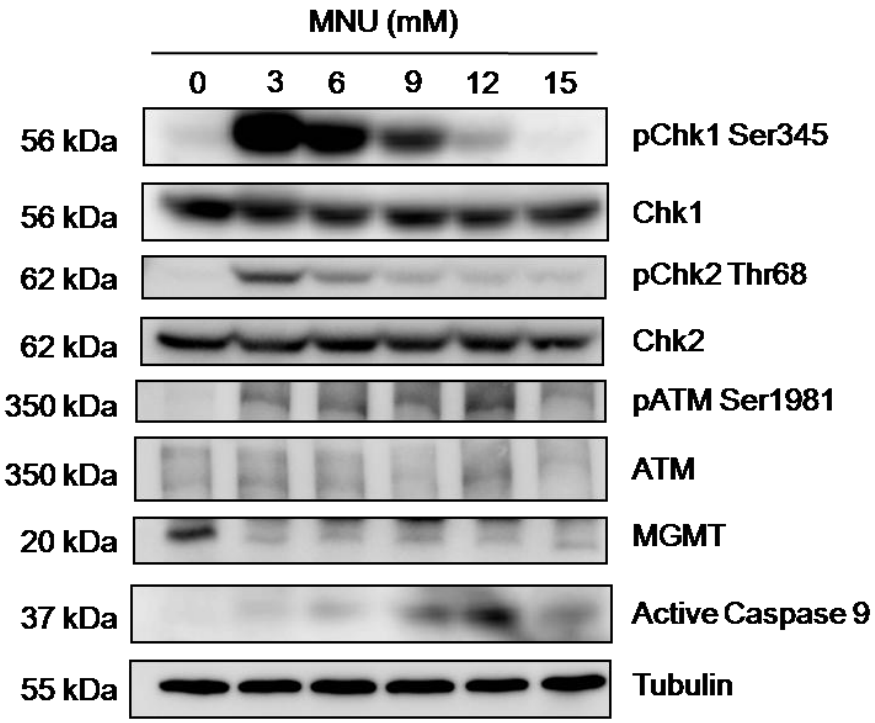

Figure 4. MNU-induced activation of cell cycle checkpoint proteins at high doses. MCF7 cells were treated with MNU concentrations ranging between 3 mM and 15 mM for 2 hours. Cell lysates were analyzed for activation of cell cycle checkpoint regulators, levels of MGMT and active caspase 9 using immunoblot analysis. Immunoblots are representative of two independent sets of experiments. Approximate molecular weights are indicated on the left of corresponding blots.

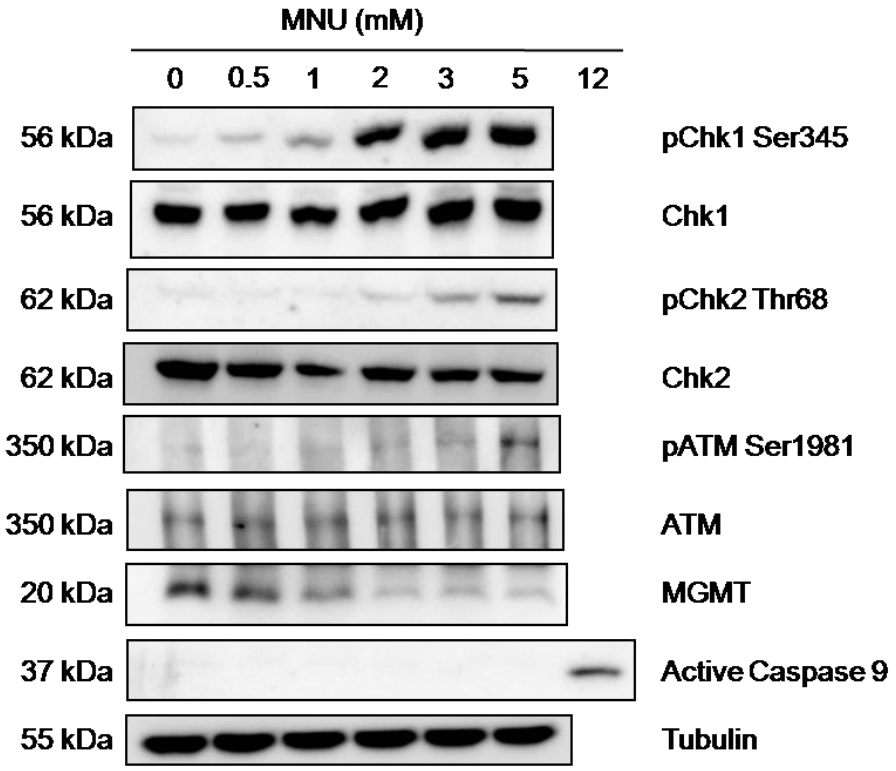

Figure 5. MNU-induced activation of cell cycle checkpoint proteins at low doses. MCF7 cells were treated with MNU concentrations ranging between 0.5 mM and 5 mM for 2 hours. Cell lysates were analyzed for activation of cell cycle checkpoint regulators, levels of MGMT and active caspase 9 using immunoblot analysis. Lysate from MCF7 cells treated with 12 mM MNU was used as positive control for activation of caspase 9. Immunoblots are representative of two independent sets of experiments. Approximate molecular weights are indicated on the left of corresponding blots.

MNU-induced checkpoint activation is dependent on MGMT levels

To investigate the dependence of MNU-induced checkpoint activation on levels of MGMT in cells, MCF10A cells (normal mammary epithelial origin) were treated with MNU concentrations ranging between 0.5 mM and 5 mM. MCF10A cells express much lower levels of MGMT with respect to MCF7 cells (Figure **6**). In contrast to checkpoint activation profile in MCF7 cells, Chk1 phosphorylation was detected in MCF10A cells at the lowest concentration of MNU used (0.5 mM; Figure **6**). Interestingly, the lowest MNU dose at which ATM and Chk2 phosphorylation were detected (3 mM) was the same for MCF7 and MCF10A cells (Figure **5** and Figure **6**).

To investigate MNU-induced checkpoint activation profile in MCF7 cells expressing lower levels of functional MGMT protein, cells were treated with an MGMT inhibitor (O6-BG) prior to treatment with MNU. MGMT inhibition did not result in any significant change in the activation profile of sensor and effector checkpoint kinases after 5 mM MNU treatment (Figure **7**). On comparing the checkpoint activation profile of MCF7 cells at different doses of MNU (0.5 mM and 5 mM), it was observed that MGMT depletion resulted in the activation of effector kinases, Chk2 and Chk1, at the lowest MNU dose (0.5 mM; Figure **8**). However no considerable difference was detected in the MNU dose-dependent activation profile of the sensor kinase ATM after MGMT depletion (Figure **8**).

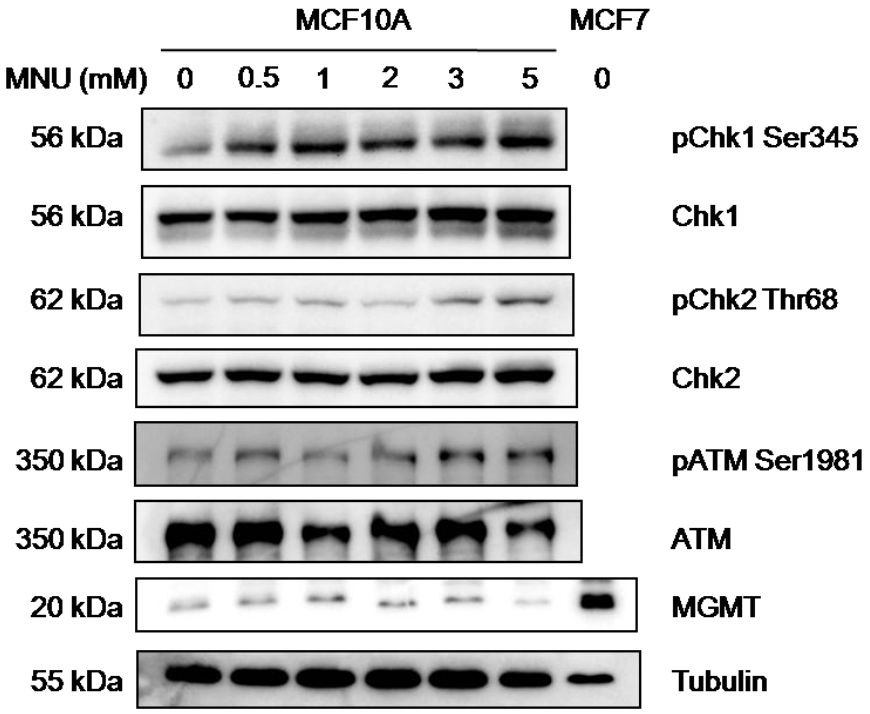

Figure 6. MNU-induced activation of cell cycle checkpoint proteins in MCF10A. MCF10A cells were treated with MNU concentrations ranging between 0.5 mM and 5 mM for 2 hours. Cell lysates were analyzed for activation of cell cycle checkpoint regulators and levels of MGMT using immunoblot analysis. Untreated MCF7 lysate was used to compare MGMT levels across cell lines. Immunoblots are representative of two independent sets of experiments. Approximate molecular weights are indicated on the left of corresponding blots.

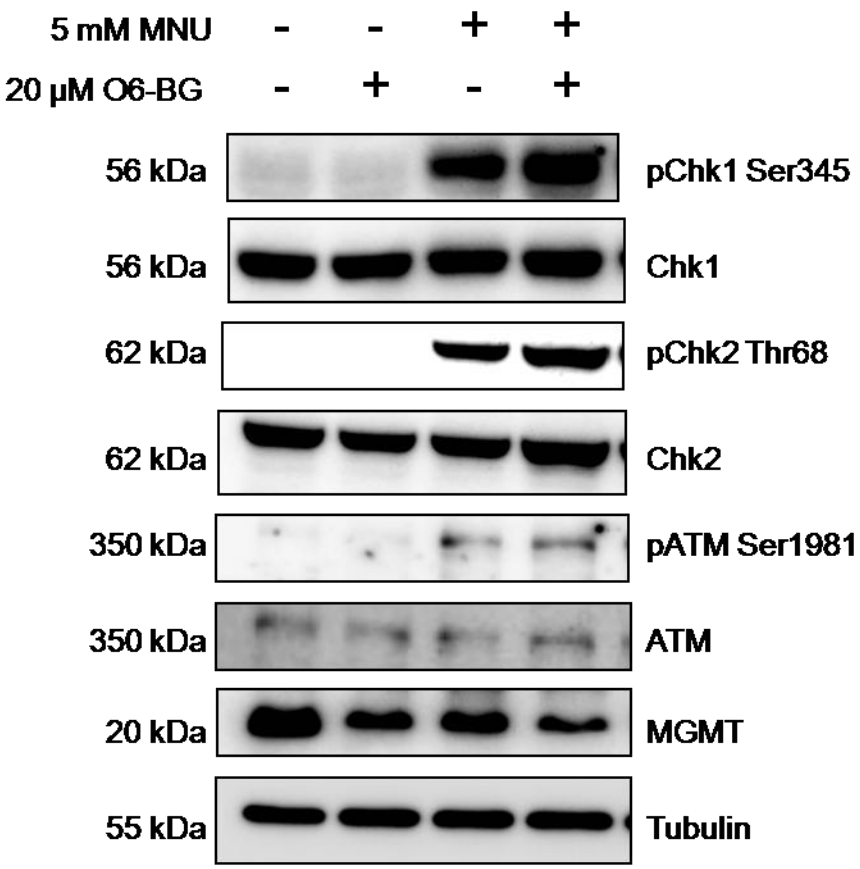

Figure 7. MNU-induced checkpoint activation in MCF7 after MGMT depletion. MCF7 cells were incubated with 20 µM O6-BG for 1 hour prior to treatment with 5 mM MNU for 2 hours. Cell lysates were analyzed for activation of cell cycle checkpoint regulators and levels of MGMT using immunoblot analysis. Immunoblots are representative of one set of experiment. Approximate molecular weights are indicated on the left of corresponding blots.

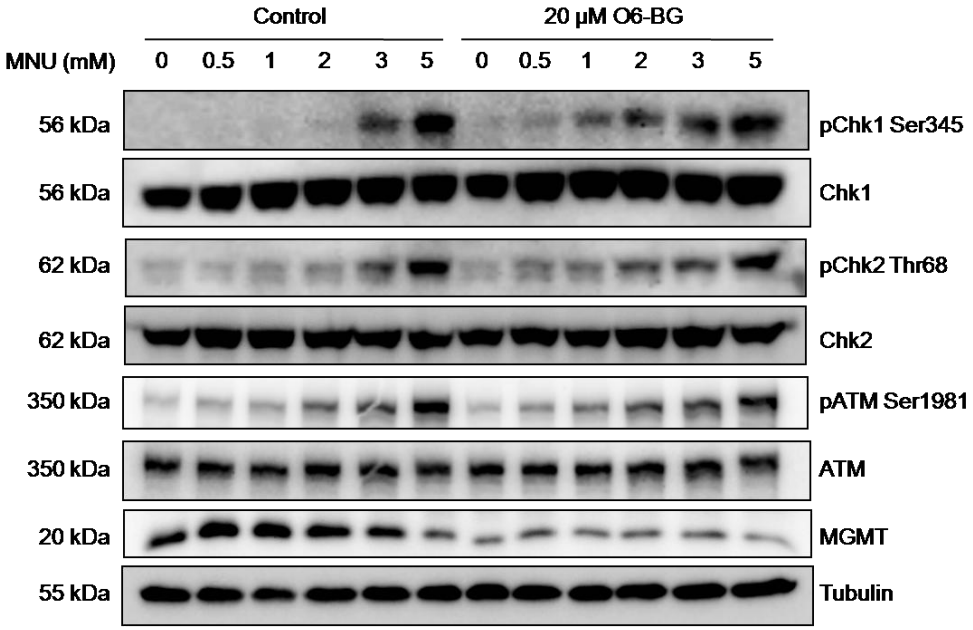

Figure 8. Checkpoint activation in MCF7 at low MNU doses post-MGMT depletion. MCF7 cells were incubated with 20 μM O6-BG for 1 hour prior to treatment with MNU concentrations ranging between 0.5 mM and 5 mM for 2 hours. Cell lysates were analyzed for activation of cell cycle checkpoint regulators and levels of MGMT using immunoblot analysis. Immunoblots are representative of two independent sets of experiments. Approximate molecular weights are indicated on the left of corresponding blots.

Chk2 activation precedes Chk1 activation for NEU, but not MNU, induced damage

To elucidate the temporal profile of MNU-induced activation of checkpoint proteins, time course assay was performed in MCF7 cells after treatment with 5 mM MNU. The sensor kinase ATM and the downstream effector kinases, Chk2 and Chk1, were phosphorylated after 10 minutes of MNU treatment (Figure 9). The degree of phosphorylation for Chk2 and Chk1 showed an increase from 10 minutes to 20 minutes and this level was sustained till 120 minutes post-MNU treatment (Figure 9). A previous study had shown that after MCF7 cells were treated with a DNA ethylating agent, N-nitroso-N-ethylurea (NEU), which differs in structure from MNU only at the alkyl residue, ATM and Chk2 phosphorylation preceded Chk1 phosphorylation (data unpublished). We studied the temporal profile of checkpoint activation post-NEU damage in HeLa cells (a cell line of cervical cancer origin) and found similar results as were obtained with MCF7 cells. ATM and Chk2 phosphorylation were detected at 10 minutes and Chk1 phosphorylation was detected at 30 minutes after treatment with 10 mM NEU (Figure 10).

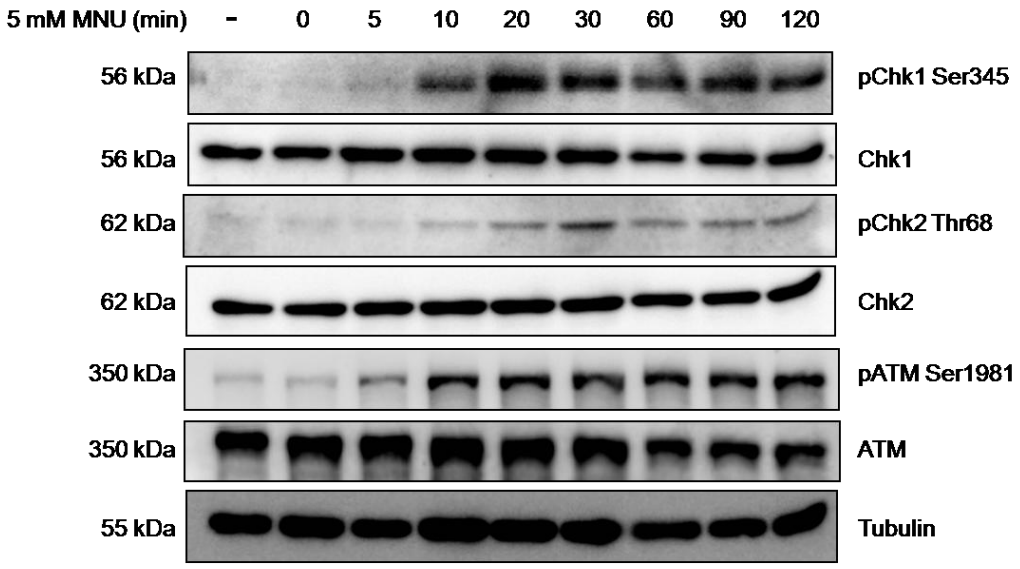

Figure 9. Time course analysis of checkpoint activation in MCF7 after MNU-induced damage. MCF7 cells were treated with 5 mM MNU for time periods ranging from 0 minutes to 2 hours before harvesting. Cell lysates were analyzed for activation of cell cycle checkpoint regulators using immunoblot analysis. Immunoblots are representative of three independent sets of experiments. Approximate molecular weights are indicated on the left of corresponding blots.

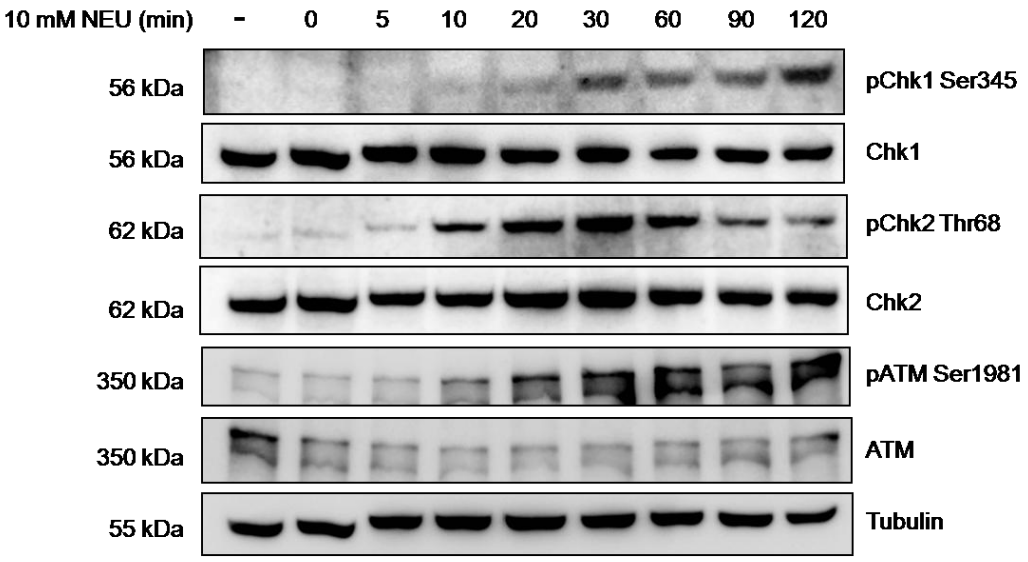

Figure 10. Time course analysis of checkpoint activation in HeLa after NEU-induced damage. HeLa cells were treated with 10 mM NEU for time periods ranging from 0 minutes to 2 hours before harvesting. Cell lysates were analyzed for activation of cell cycle checkpoint regulators using immunoblot analysis. Immunoblots are representative of three independent sets of experiments. Approximate molecular weights are indicated on the left of corresponding blots.

ATM and DNA-PK are not required for Chk1 activation after NEU damage

In order to investigate whether ATM and Chk2 activation are required for Chk1 phosphorylation following NEU treatment, a small molecule inhibitor of ATM auto-phosphorylation, KU 55933, was used to prevent activation of ATM and its downstream targets (including Chk2) after inducing NEU damage. DMNB, an inhibitor of DNA-PK, was also used in this experiment since it is known that members of PIKK family of kinases show functional redundancy in ATM-deficient cells (Tomimatsu et al., 2009). Chk1 phosphorylation after 10 mM NEU treatment was not ablated after ATM or DNA-PK inhibition or a combination of both (Figure **11**).

To elucidate whether inhibiting ATM and Chk2 phosphorylation affects the temporal profile of Chk1 phosphorylation post-NEU damage, a time course assay was performed in MCF7 cells after NEU treatment in the presence of KU 55933. Interestingly, though Chk2 phosphorylation was almost completely abolished, Chk1 phosphorylation was detected 20 minutes post-damage (Figure **12**).

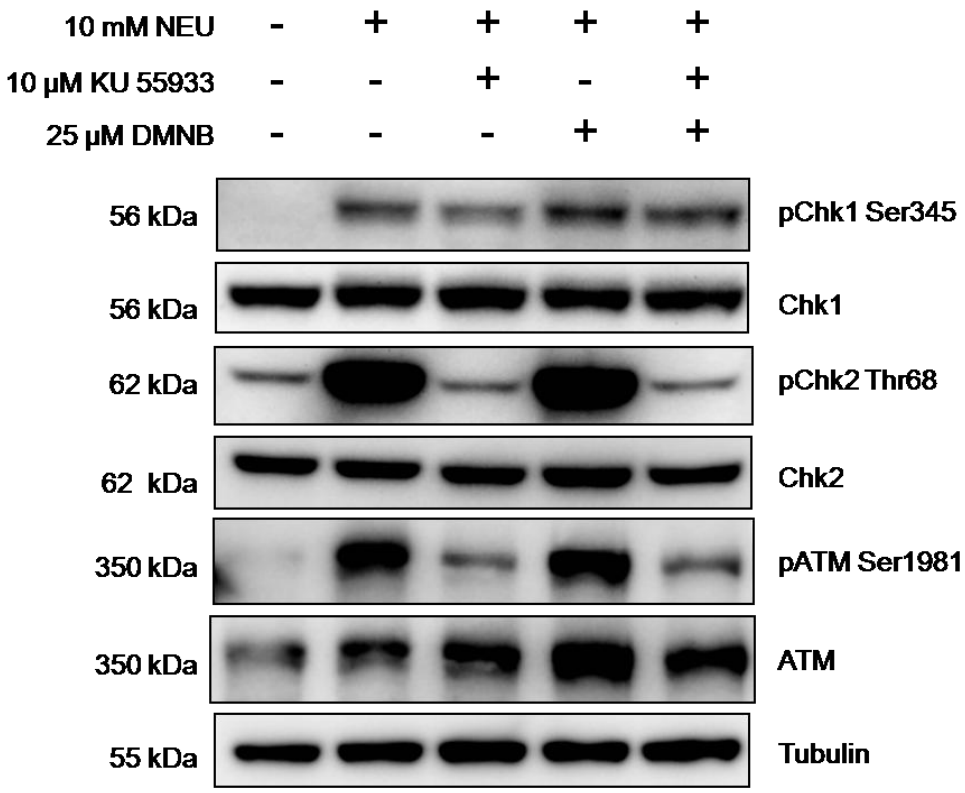

Figure 11. Checkpoint activation in MCF7 after NEU damage in presence of ATM and DNA-PK inhibition. MCF7 cells were incubated with 10 µM KU 55933 and/on 25 µM DMNB immediately prior to treatment with 10 mM NEU for 2 hours. Cell lysates were analyzed for activation of cell cycle checkpoint regulators using immunoblot analysis. Immunoblots are representative of two independent sets of experiments. Approximate molecular weights are indicated on the left of corresponding blots.

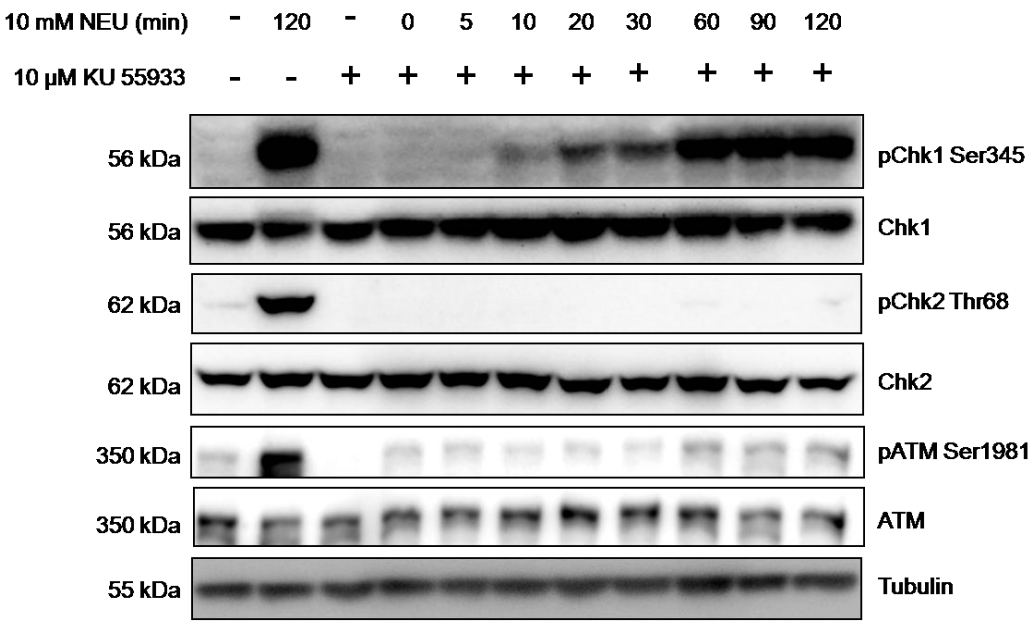

Figure 12. Time course analysis of checkpoint activation in MCF7 after NEU damage in the presence of ATM inhibition. MCF7 cells were incubated with 10 µM KU 55933 immediately prior to treatment with 10 mM NEU for time periods ranging from 0 minutes to 2 hours before harvesting. Cell lysates were analyzed for activation of cell cycle checkpoint regulators using immunoblot analysis.

3D on-top culture of MCF10A as a model to study MNU-induced breast cancer

3D on-top culture of MCF10A cells was developed to obtain a model to study the morphological architecture of human mammary gland *in vitro*. Following 10 days of growth in basement membrane culture, MCF10A cells formed multicellular acini-like spheroids which represented the layer of basal epithelial cells surrounding a hollow lumen in a lobule of human mammary gland (Figure **13**). To investigate whether cells forming these hollow spheroids retained apicobasal polarization as observed in human glandular epithelium, the acinar structures were immunostained in order to visualize the localization of α6 integrin, a transmembrane extracellular matrix (ECM) receptor which is a marker of interaction with basement membrane. We observed strong basal localization (with weak lateral staining) of α6 integrin in the equatorial cross sections of a Day 10 MCF10A acinus (Figure **14**). Therefore, the 3D on-top cultures recapitulated key morphological features of the breast epithelium *in vivo* which includes formation of acini-like spheroids with a hollow lumen and apico-basal polarization of cells forming these structures.

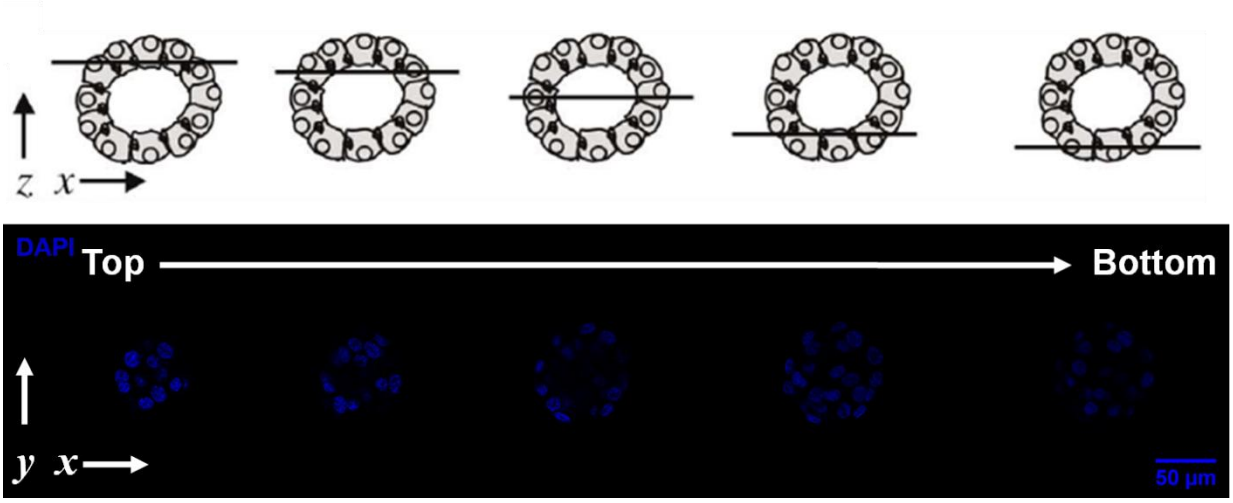

Figure 13. Representative confocal microscopic imaging of MCF10A acinus. DAPI-stained (blue) cross sections (*x*-*y* axis) of a Day 10 MCF10A acinus. Schematic representation on top of each section corresponds to its relative position along the *z* axis.

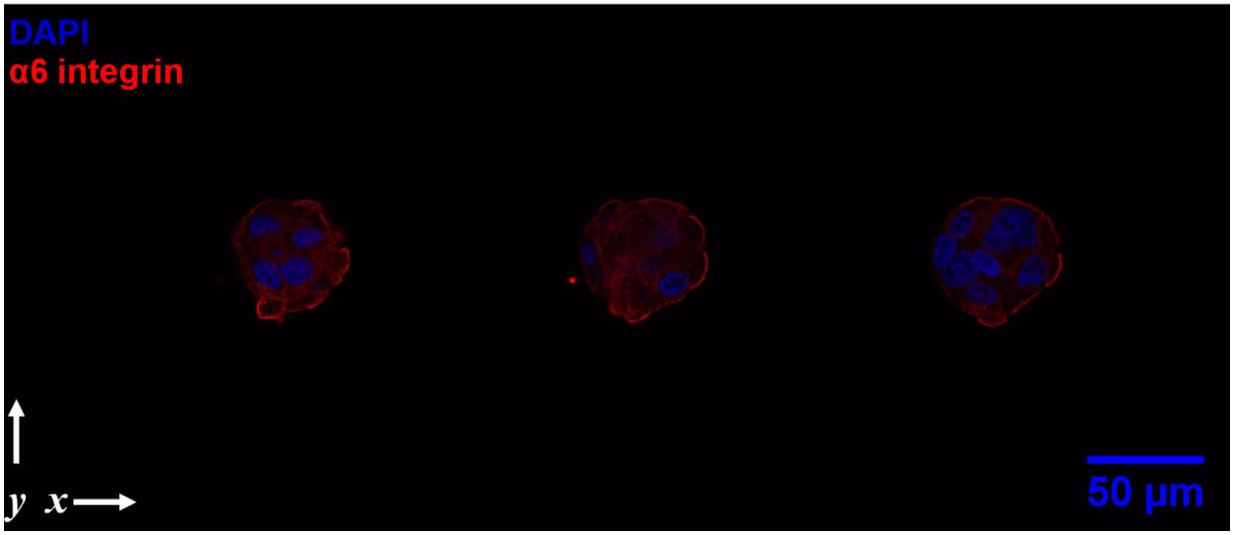

Figure 14. Day 10 MCF10A acinus immunostained with α6 integrin antibody. MCF10A cells were grown as 3D-on top cultures for 10 days and were stained with DAPI (blue) to visualize nuclei and with antibody towards α6 integrin (red) to delineate its attachment with basement membrane. Serial cross sections (from left to right) correspond to roof, equator and floor of the acinar structure.

Discussion

DNA alkylating agents do not directly induce breaks in the genome, however the intermediates generated during processing of the modified nucleotides activate DNA damage repair pathways (Roos et al., 2009). In this study, we have shown that brief exposure to a monofunctional DNA methylating agent, MNU, causes more than 75% cell mortality in MCF7 cells at sub-millimolar doses (**Figure 3**). Interestingly, at these MNU concentrations, the activation of terminal caspase 9 occurred in absence of the phosphorylation of effector kinases, Chk2 and Chk1 (**Figure 4**). The initiation of apoptosis is possibly triggered by the direct phosphorylation of p53 at serine-15 residue by ATM in response to DNA alkylation damage, as reported previously (Adamson et al., 2002). Since only a few studies have shown activation of the ATM kinase immediately after exposure to DNA methylating agents, the exact mechanism of this response has not yet been resolved. One hypothesis states that processing of closely spaced O^6meG lesions on opposite strands of DNA might lead to generation of a DSB, which possibly elicits activation of the ATM kinase (Stojic et al., 2004). However this view needs to be substantiated by biochemical and live imaging studies.

It is established that the suicidal repair protein MGMT reverses the cytotoxicity of O^6meG lesions and mammalian tissues expressing higher levels of MGMT are more resistant to deleterious effects of S_N1 type DNA methylating agents (Kaina et al., 2010). Our findings provide direct evidence of an inverse correlation between cellular levels of functional MGMT protein and the extent of phosphorylation of effector kinases of the DNA damage response pathways. MGMT depletion in MCF7 cells using a pseudosubstrate resulted in activation of checkpoint regulators at a much lower MNU dose in comparison to cells treated with MNU alone (**Figure 8**). This finding has to be further strengthened by MGMT overexpression studies to conclude that the level of functional MGMT protein is the sole factor which decides the MNU dose beyond which DNA damage response is initiated in mammalian cells. Moreover it will be interesting to investigate whether the irreversibly inactivated form of this DNA repair enzyme acts as a

direct indicator of genomic instability induced by alkylating agents and thus recruits signaling proteins of alternative repair pathways at the damage sites.

Though it is not known if the single stranded gaps generated at higher doses of DNA alkylating agents act as a precursor for DSBs or vice versa, we have shown that the temporal dynamics of DNA damage checkpoint activation varies even for nitroso compounds derived from the same structural backbone. For the ethylating agent NEU, the kinase downstream of ATM, Chk2, was phosphorylated prior to Chk1 activation while both effector kinases, Chk2 and Chk1, were phosphorylated at the same time point after MNU-induced damage (**Figure 9** and **Figure 10**). The temporal profile of NEU-induced checkpoint activation is similar to a previous study in which IR-induced damage resulted in an ATM–to–ATR switch orchestrated via a single-stranded intermediate (Shiotani and Zou, 2009). However it is unlikely that repair of O^6EtG lesions involves a DSB resection step since Chk1 phosphorylation was not compromised after complete ablation of ATM autophosphorylation using a selective inhibitor of ATM kinase activity (**Figure 12**). Since response of individual cells in an asynchronous culture might differ from the population response obtained in immunoblot analysis, cell synchronization experiments are required to resolve if the nature of damage induced by NEU is cell cycle phase-dependent.

Finally, the MCF10A model of human glandular epithelium can be used as a powerful tool to investigate immediate effects of DNA alkylating agents on mammary tissue architecture. Formation of acinus-like structures in three dimensional basement membrane culture recapitulates numerous crucial steps in epithelial tissue morphogenesis, such as proliferation and apico-basal polarization of cells during early stages and growth arrest and apoptosis of luminal cells at later stages of development (Debnath et al., 2003). Analogous to the MNU-induced rat mammary tumor model, exposure to alkylating agents during early stages of development might predispose MCF10A acini to impairment of epithelial cell differentiation and failure to induce luminal cell death, which are hallmarks of early oncogenesis in breast tissue (Huang and Ip, 2001; Puertollano et al., 2008; Sharma et al., 2011).

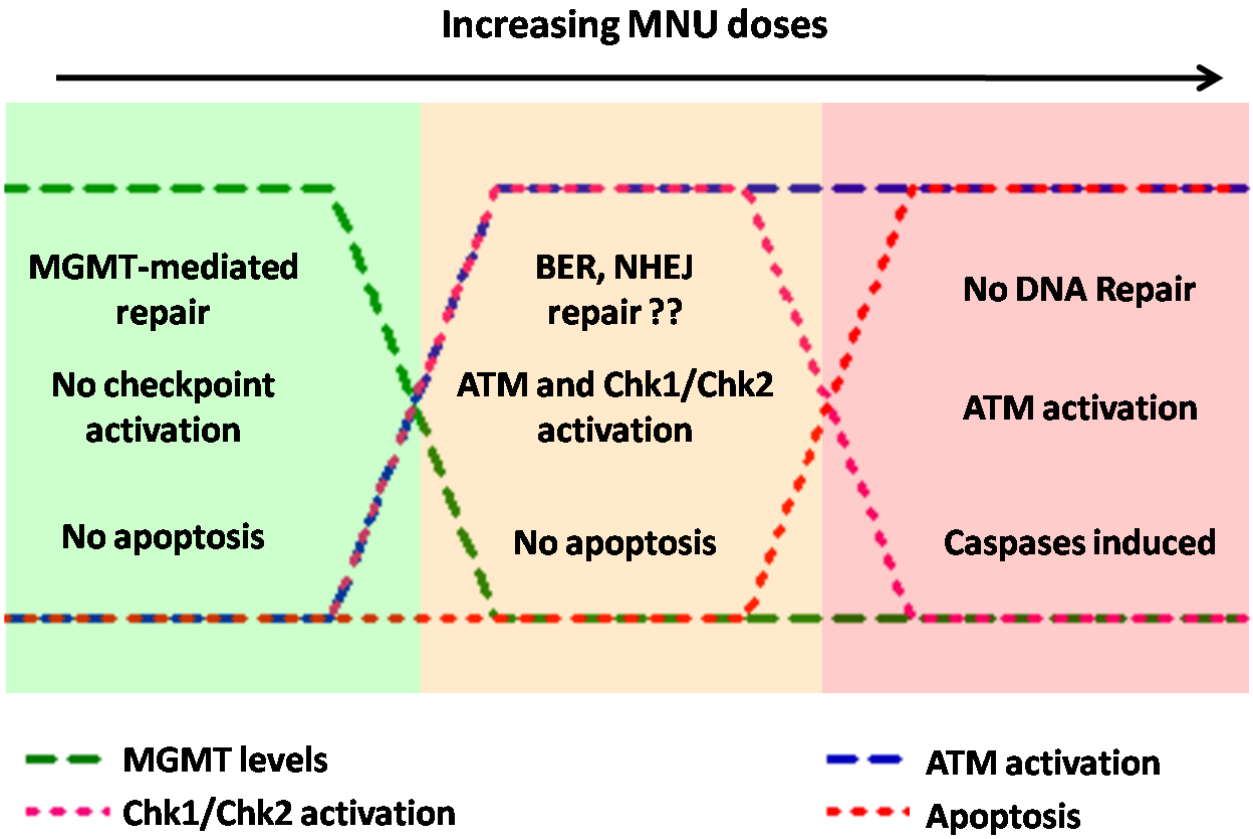

Figure 15. Proposed model for differential response of mammalian cells at different dose ranges of MNU-induced damage. At low doses of MNU, MGMT-mediated repair of O^6meG lesions prevents activation of DNA damage checkpoint. Endogenous MGMT is depleted at intermediate MNU doses and checkpoint proteins are activated due to formation of DNA strand breaks. Alternative repair mechanisms such as base excision repair (BER) and non-homologous end joining (NHEJ) are recruited in this dose range for repair of damage induced at O^6meG lesion sites. At high doses of MNU, apoptosis is initiated by activation of caspases without eliciting the activation of effector kinases of the DNA damage checkpoint signaling cascade.

Modulation of activity of a single gene or a small subset of genes has been shown to be sufficient for disruption of polarized MCF10A acinar structure (Chen et al., 2010; Henry et al., 2011; Guo et al., 2010). However since breast tumors in humans are highly heterogenous in their genetic makeup and response to therapy, identifying critical steps during early progression of MNU-induced mammary oncogenesis using the MCF10A model can provide new insights for designing more efficient strategies to combat genetically diverse carcinomas in women.

References

Adams, K. E., Medhurst, A. L., Dart, D. A., and Lakin, N. D. (2006). Recruitment of ATR to sites of ionising radiation-induced DNA damage requires ATM and components of the MRN protein complex. Oncogene *25*, 3894–3904.

Adamson, A. W., Kim, W. J., Shangary, S., Baskaran, R., and Brown, K. D. (2002). ATM is activated in response to N-methyl-N'-nitro-N-nitrosoguanidine-induced DNA alkylation. The Journal of Biological Chemistry *277*, 38222–38229.

Chan, M. M., Lu, X., Merchant, F. M., Iglehart, J. D., and Miron, P. L. (2005). Gene expression profiling of NMU-induced rat mammary tumors: cross species comparison with human breast cancer. Carcinogenesis *26*, 1343–1353.

Chen, J., Miller, E. M., and Gallo, K. A. (2010). MLK3 is critical for breast cancer cell migration and promotes a malignant phenotype in mammary epithelial cells. Oncogene *29*, 4399–4411.

Christmann, M., and Kaina, B. (2000). Nuclear translocation of mismatch repair proteins MSH2 and MSH6 as a response of cells to alkylating agents. The Journal of Biological Chemistry *275*, 36256–36262.

Ciccia, A., and Elledge, S. J. (2010). The DNA damage response: making it safe to play with knives. Molecular Cell *40*, 179–204.

Cimprich, K. A., and Cortez, D. (2008). ATR: an essential regulator of genome integrity. Nature Reviews Molecular Cell Biology *9*, 616–627.

Debnath, J., Muthuswamy, S. K., and Brugge, J. S. (2003). Morphogenesis and oncogenesis of MCF-10A mammary epithelial acini grown in three-dimensional basement membrane cultures. Methods *30*, 256–268.

Engelbergs, J., Thomale, J., and Rajewsky, M. F. (2000). Role of DNA repair in carcinogen-induced ras mutation. Mutation Research *450*, 139–153.

Fu, D., Calvo, J. A., and Samson, L. D. (2012). Balancing repair and tolerance of DNA damage caused by alkylating agents. Nature Reviews Cancer, 104–120.

Guo, H. B., Johnson, H., Randolph, M., Nagy, T., Blalock, R., and Pierce, M. (2010). Specific posttranslational modification regulates early events in mammary carcinoma formation. PNAS *107*, 21116–21121.

Helt, C. E., Cliby, W. A., Keng, P. C., Bambara, R. A., and O'Reilly, M. A. (2005). Ataxia telangiectasia mutated (ATM) and ATM and Rad3-related protein exhibit selective target specificities in response to different forms of DNA damage. The Journal of Biological Chemistry *280*, 1186–1192.

Henry, L. a, Johnson, D. a, Sarrió, D., Lee, S., Quinlan, P. R., Crook, T., Thompson, a M., Reis-Filho, J. S., and Isacke, C. M. (2011). Endoglin expression in breast tumor cells suppresses invasion and metastasis and correlates with improved clinical outcome. Oncogene *30*, 1046–1058.

Huang, R.-Y., and Ip, M. M. (2001). Differential expression of integrin mRNAs and proteins during normal rat mammary gland development and in carcinogenesis. Cell and Tissue Research *303*, 69–80.

Jazayeri, A., Falck, J., Lukas, C., Bartek, J., Smith, G. C. M., Lukas, J., and Jackson, S. P. (2006). ATM- and cell cycle-dependent regulation of ATR in response to DNA double-strand breaks. Nature Cell Biology *8*, 37–45.

Kaina, B., Margison, G. P., and Christmann, M. (2010). Targeting O^6-methylguanine-DNA methyltransferase with specific inhibitors as a strategy in cancer therapy. Cellular and Molecular Life Sciences *67*, 3663–3681.

Klapacz, J., Meira, L. B., Luchetti, D. G., Calvo, J. A., Bronson, R. T., Edelmann, W., and Samson, L. D. (2009). O(6)-methylguanine-induced cell death involves exonuclease 1 as well as DNA mismatch recognition in vivo. PNAS *106*, 576–581.

Kondo, N., Takahashi, A., Ono, K., and Ohnishi, T. (2010). DNA damage induced by alkylating agents and repair pathways. Journal of Nucleic Acids *2010*, 543531.

Lee, G. Y., Kenny, P. A., Lee, E. H., and Bissell, M. J. (2007). Three-dimensional culture models of normal and malignant breast epithelial cells. Nature Methods *4*, 359–365.

Liu, Y., Fang, Y., Shao, H., Lindsey-Boltz, L., Sancar, A., and Modrich, P. (2010). Interactions of human mismatch repair proteins MutSalpha and MutLalpha with proteins of the ATR-Chk1 pathway. The Journal of Biological Chemistry *285*, 5974–5982.

Puertollano, M. A., Carrera, M. P., Puertollano, E., de Cienfuegos, G. Á., RamÍrez-ExpÓsito, M. J., de Pablo, M. A., and MartÍnez-Martoz, J. M. (2008). Analysis of caspase activities in rat mammary tumours induced by N-methyl-nitrosourea. Oncology Reports *20*, 657–662.

Roos, W. P., Nikolova, T., Quiros, S., Naumann, S. C., Kiedron, O., Zdzienicka, M. Z., and Kaina, B. (2009). Brca2/Xrcc2 dependent HR, but not NHEJ, is required for protection against O(6)-methylguanine triggered apoptosis, DSBs and chromosomal aberrations by a process leading to SCEs. DNA Repair *8*, 72–86.

Russo, J., and Russo, I. H. (2000). Atlas and histologic classification of tumors of the rat mammary gland. Journal of Mammary Gland Biology and Neoplasia *5*, 187–200.

Sharma, D., Smits, B. M. G., Eichelberg, M. R., Meilahn, A. L., Muelbl, M. J., Jill, D., and Gould, M. N. (2011). Quantification of Epithelial Cell Differentiation in Mammary Glands and Carcinomas from DMBA- and MNU-Exposed Rats. Carcinogenesis *6*, e26145.

Shiloh, Y. (2006). The ATM-mediated DNA-damage response: taking shape. Trends in Biochemical Sciences *31*, 402–410.

Shiotani, B., and Zou, L. (2009). Single-stranded DNA orchestrates an ATM-to-ATR switch at DNA breaks. Molecular Cell *33*, 547–558.

Shrivastav, N., Li, D., and Essigmann, J. M. (2010). Chemical biology of mutagenesis and DNA repair: cellular responses to DNA alkylation. Carcinogenesis *31*, 59–70.

Stojic, L., Brun, R., and Jiricny, J. (2004). Mismatch repair and DNA damage signalling. DNA Repair *3*, 1091–1101.

Takahashi, H., Uemura, Y., Nakao, I., and Tsubura, A. (1995). Induction of mammary carcinomas by the direct application of crystalline N-methyl-N-nitrosourea onto rat mammary gland. Cancer Letters *92*, 105–111.

Tomimatsu, N., Mukherjee, B., and Burma, S. (2009). Distinct roles of ATR and DNA-PKcs in triggering DNA damage responses in ATM-deficient cells. EMBO Reports *10*, 629–635.

Xu-Welliver, M., and Pegg, A. E. (2002). Degradation of the alkylated form of the DNA repair protein, O6-alkylguanine-DNA alkyltransferase. DNA Repair *23*, 823–830.